Materials Research Express

ACCEPTED MANUSCRIPT

Highly Phosphorescent Hollow Fibers Inner-coated with Tungstate Nanocrystals

To cite this article before publication: Pui Fai Ng *et al* 2017 *Mater. Res. Express* in press https://doi.org/10.1088/2053-1591/aa8ebd

Ng, P. F., Bai, G., Si, L., Lee, K. I., Hao, J., Xin, J. H., & Fei, B. (2017). Highly phosphorescent hollow fibers inner-coated with tungstate nanocrystals. Materials Research Express, 4(12), 125029.

Highly Phosphorescent Hollow Fibers Inner-coated with Tungstate Nanocrystals

Pui Fai Ng [1], Gongxun Bai [2], Liping Si [1], Ka I Lee [1], Jianhua Hao [2], Bin Fei [1,]*

1. Nanotechnology Center, Institute of Textiles & Clothing, Hong Kong Polytechnic University, Hong Kong, China.

2. Department of Applied Physics, Hong Kong Polytechnic University, Hong Kong, China.

* Corresponding author. E-mail: tcfeib@polyu.edu.hk. Tel: 00852 - 2766 4795.

KEYWORDS

tungstate nanocrystal, phosphorescence, biomimetic mineralization, kapok fiber, hydrothermal synthesis

ABSTRACT

In order to develop luminescent microtubes from natural fibers, a facile biomimetic mineralization method was designed to introduce the $CaWO_4$-based nanocrystals into kapok lumens. The structure, composition, and luminescence properties of resultant fibers were investigated with microscopes, X-ray diffraction, thermogravimetric analysis, and fluorescence spectrometry. The yield of tungstate crystals inside kapok was significantly promoted with a process at high temperature and pressure – the hydrothermal treatment. The tungstate crystals grown on the inner wall of kapok fibers showed the same crystal structure with those naked powders, but smaller in crystal size. The resultant fiber assemblies demonstrated reduced phosphorescence intensity in comparison to the naked tungstate powders. However, the fibers gave more stable luminescence than the naked powders in wet condition. This approach explored the possibility of decorating natural fibers with high load of nanocrystals, hinting potential applications in anti-counterfeit labels, security textiles, and even flexible and soft optical devices.

1. INTRODUCTION

One-dimensional (1D) luminous micro/nanostructures are attracting growing attention from wide range of researchers because of their potential applications in chemical sensors, optical imaging, polarized emission, and optoelectronic devices.[1-4] In principle, the 1D fluorescent nanostructures can be fabricated by supramolecular assemblies of organic chromophores or template-directed crystal growth.[5-9] Higher scale 1D fluorescent structures are difficult to

obtain directly from single component, although they are essential to the fabrication of flexible and soft optoelectronic devices. In order to obtain freestanding and flexible luminescent microfibers in large scale, the most widely used method is hybridizing luminescent units with suitable matrix/gelators.[10-12] In literature, electrospinning, dry/wet spinning and melt extrusion have been reported to manufacture the luminescent microfibers from ready-for-use luminous nanoparticles and suitable polymers.[13-17] However, the incorporation of inorganic luminous particles usually deteriorate the polymer mechanical properties and the achievable amount of fillers in the polymer fibers is very limited (usually below 20 wt%). When the luminous materials randomly distribute in the whole polymer matrix, their luminescence intensity was greatly suppressed by the absorption and scattering effects. Controlled distribution of high amount of luminescent crystals within flexible fibers is still in demand.

Biomimetic mineralization is a versatile method to develop hierarchical hybrid structures.[18-20] This approach has rarely been used to manufacture fluorescent materials. Although rare-earth up-converting nanoparticles have been grafted onto nanocellulose template, the luminescent nanoparticles were synthesized separately and modified with organic ligands before deposition, and the grafting amount was still low.[21] Here, we directly use a natural hollow fiber - kapok fiber - as template and inorganic salts as starting materials, to manufacture strongly luminous microfibers with high load of metal tungstate nanocrystals by one-pot synthesis. Metal tungstate is an important family of inorganic phosphorescent materials that have been widely applied in fluorescent lamps, X-ray intensified screen, scintillator materials and optical fibers.[22-25] The luminescence color of anion complex WO_4^{2-} can be conveniently adjusted by doping with transition metal ions or rare-earth ions, and its luminescence efficiency can be improved by doping with alkaline metal ions.[26-28]

Kapok fiber is a natural plant fiber with large lumen and low density. Its wall is as thin as 1.0 μm, and the inherent cutin on its outer surface offers the fiber a silky gloss with hydrophobicity and oleophilicity.[29] All of these unique characteristics endow kapok fibers extensive applications in pillow stuffing, buoyancy material, oil sorbent, oil / water separation and metal ion sorbent.[30-34] However, kapok fiber has not been well studied for luminous applications, although fluorescent dyes and particles have been filled into kapok fibers for special effects.[35] This work provides a promising alternative approach for preparing freestanding and flexible luminous microtubes that can be easily manipulated into devices and textiles for sensing and alarming applications.

2. EXPERIMENTAL SECTION

2.1. Materials.

Anhydrous calcium chloride (96%), europium(III) oxide (99.99%), and sodium tungstate dihydrate (99%) were all purchased from Sigma-Aldrich. Nitric acid aqueous solution (69%) and anhydrous citric acid (99.5%) were obtained from Fisher Scientific. All chemicals were used as received without further purification. Raw kapok fiber was supplied by Shanghai Dingcheng Biotechnology Co., Ltd., China.

2.2. Mineralization of Tungstate phosphors in Kapok Fibers.

Stoichiometric amount of raw materials were measured to obtain a Ca / Eu / W molar ratio of 0.975 : 0.025 : 1. Eu_2O_3 of 0.044 g was dissolved into 20 ml of 10% HNO_3 solution on heating for introducing Eu^{3+}. The above solution was mixed and fully stirred with 1.050 g $CaCl_2$ and 2.1 g citric acid at room temperature. $Na_2WO_4 \cdot H_2O$ of 3.300 g was gradually added into the mixed solution, followed by NaOH addition for neutralization. The total volume of the solution was

controlled at 60 ml. Kapok fibers of 0.500 g were introduced into the neutral solution by sonication for half an hour to allow solution penetration. The neutral solution was then adjusted to pH 9 to give a white homogeneous dispersion. Further mineralization was performed at room temperature (25 ^{o}C) for 6 or 24 hours. The final products, which were denoted by RT-6 or RT-24, were thoroughly washed with distilled water and dried at room temperature.

The further mineralization was also carried out at 160 ^{o}C within a well-sealed Teflon-lined stainless steel autoclave of 100 ml capacity (hydrothermal deposition) instead of the room temperature mineralization, which gave products HT-6 and HT-24. Pure tungstate powders were synthesized under the same conditions for 24 hours without fiber introduction for comparison, denoted by RT and HT, respectively.

2.3. Characterization.

Fiber morphology was observed by an optical microscope (Nikon OPTIPHOT-POL, with CCD camera Leica DFC 290 HD), a reflection microscope (Nikon eclipse Ti, with UV light sources), and a field-emission scanning electron microscope (FE-SEM, JEOL Ex-64125JMU field-emission at 5 kV). X-ray diffraction (XRD) pattern was recorded on Rigaku SmartLab with Cu Kα radiation (λ = 1.54 Å) at 45 kV and 200 mA. The mineral loads of the dried fiber samples were measured using a thermogravimetric analyzer (TGA, Mettler Toledo TGA / DSC 1) at a heating rate 10 ^{o}C/min in air atmosphere. The luminescence spectra were measured on a time-resolved fluorescence spectrometer (Edinburgh FLS920 with a 450 W Xe lamp) at room temperature, which has a spectral resolution of 1 nm.

3. RESULTS AND DISCUSSION

Biomimetic mineralization allows the selective growth of inorganic crystals on organic substrates with specific surface groups. This principle was exploited to decorate an elegant natural fiber, kapok fiber, to obtain a highly luminescent microtube. The wall of kapok fiber shows hydrophilic property on inner surface and hydrophobic property on outer surface, because of its multilayer structures. The outermost layer is a wax-like cutin layer while the innermost layer is purely cellulose as born from the plant cell.[29] These two different surfaces would allow the selective nucleation of mineral crystals inside the lumen of kapok fiber. Here we selected a tungstate crystal to decorate the kapok fiber, which resulted in a phosphorescent micro light-tube.

Among the abundant tungstates, a scheelite nanostructure CaWO4 co-doped with Eu^{3+} and Na^{+} was exploited, because of its excellent luminescence properties as demonstrated by luminescence lifetimes of milliseconds, abnormally narrowed emissions and high quantum efficiency over 50%.[28] Following the synthesis procedures as described in the experimental section, a series of decorated fibers were successfully obtained. As shown in Figure 1A, the original kapok wall is very thin (~ 1.0 μm) and transparent. After being treated at room temperature for 6 or 24 hours, the kapok lumen is decorated with some tiny particles (Figure 1B and C). The fibers are filled with denser particles after the hydrothermal deposition for 6 and 24 hours (Figure 1D and E). All these filled fibers look slight reddish under the visible light, although they have different diameters varying from 10 to 40 μm. When the fiber HT-24 was put under a reflection microscope with 254 nm light source, a bright tube emitting red light was observed (Figure 1F), indicating the successful mineralization of the tungstate crystals inside the kapok fibers.

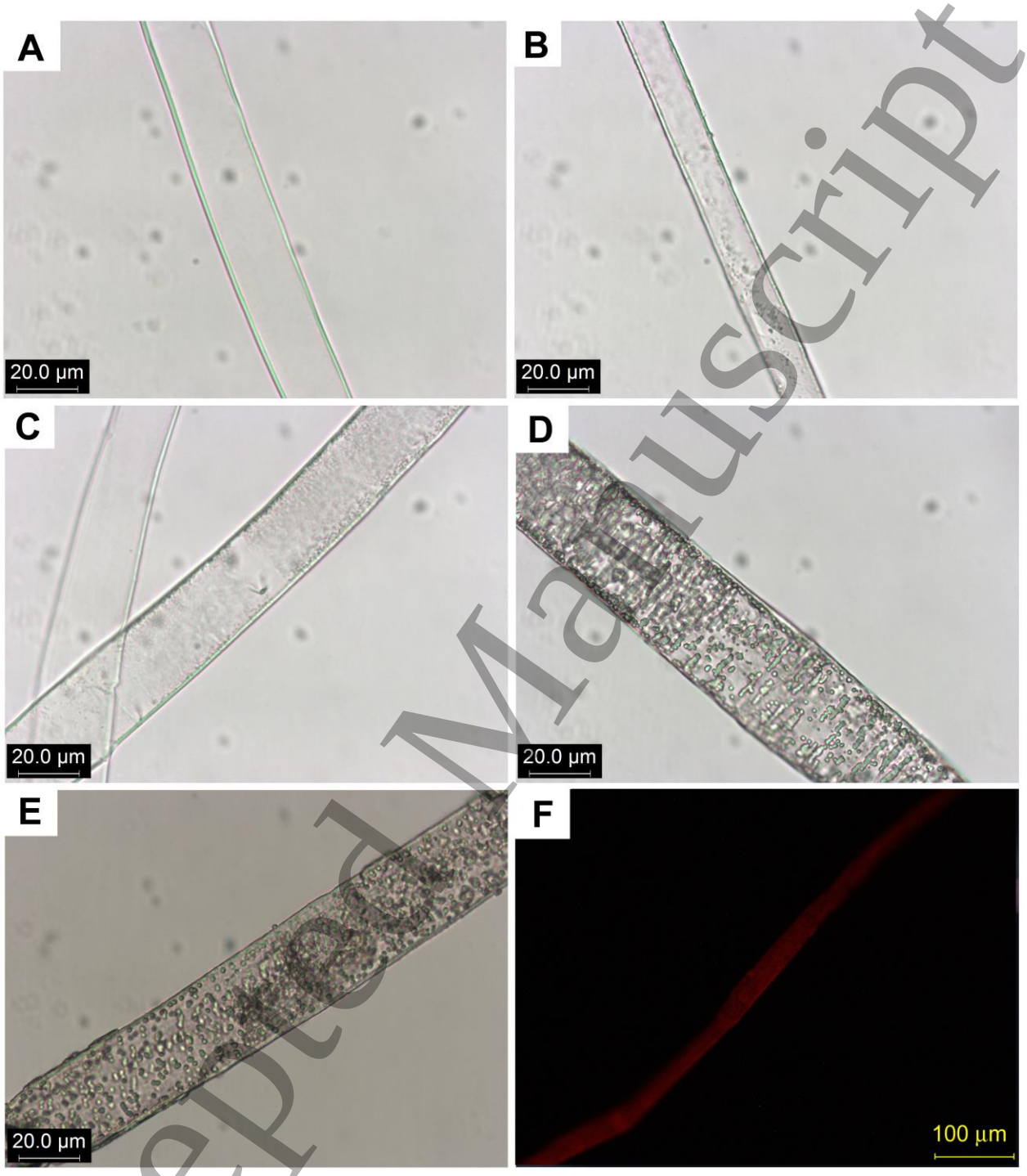

Figure 1. Microscopic images of raw and decorated kapok fibers: (A) original, (B) RT-6, (C) RT-24, (D) HT-6, (E) HT-24, and (F) HT-24 under 254 nm.

The distribution of crystals in the kapok fiber was further visualized by SEM in Figure 2. The cross-section image of raw kapok shows a wall thickness ~ 1.0 μm as well as smooth outer and inner surfaces (Figure 2A). All the decorated kapok fibers have a smooth outer surface similar to that of raw kapok and a rough inner surface with coating particles (Figure 2B-D). In comparison, the hydrothermally treated fibers present denser and thicker coatings than those treated at room temperature. The regular attachment of tungstate crystals on the inner surface was due to the selective nucleation of crystals on the hydrophilic substrate with hydroxyl groups, when the salt solution became oversaturated at a relatively high pH value. Though kapok is naturally water-resistance, the aqueous solution may still penetrate into the lumen with the assistance of sonication that drives out the air inside the fiber. The hydrothermal process induces a high pressure in the sealed canister and pumps more solution into the lumen, thus promotes mineralization on the inner wall.

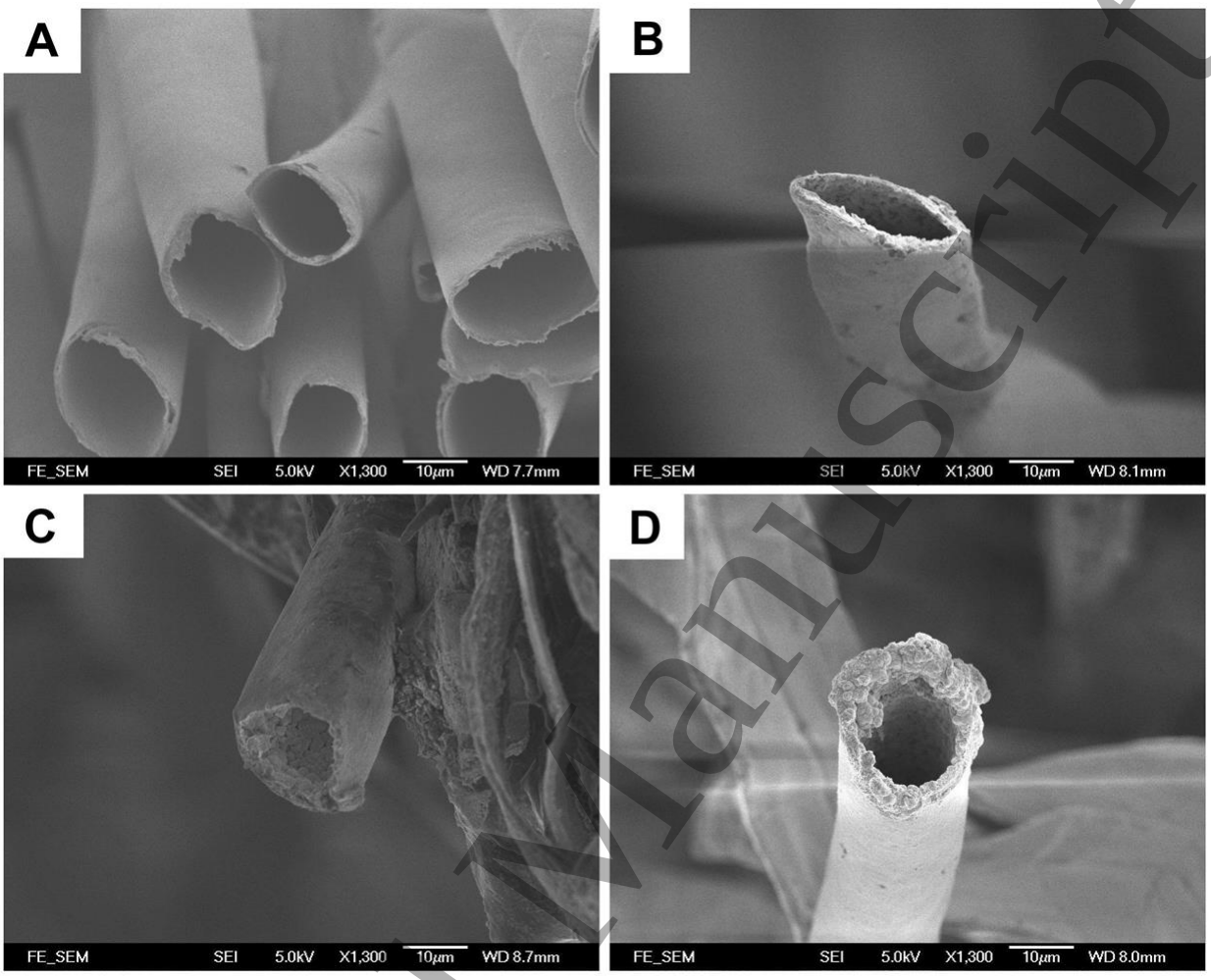

Figure 2. FE-SEM images of kapok fiber cross-sections: (A) original, (B) RT-24, (C) HT-6, (D) HT-24.

The crystal structure of mineralized tungstate was analyzed by XRD, as shown in Figure 3. The sample synthesized at room temperature presents weak and broad diffraction peaks, while the hydrothermally synthesized powders exhibit intense and narrow diffraction peaks of the standard phase, indicating that the elevation in temperature is benefitial to crystal growth. These results agree with the literature report.[28] Regarding the tungstate crystals grown in kapok lumen, they show the same trend with temperature increasing. The fibers treated at room

temperature present only a weak (112) peak in addition to the peak of original kapok while those treated at hydrothermal condition show all the diffraction peaks of standard $CaWO_4$. Notably, the peaks derived from the minerals within kapok lumen are all broader than the corresponding peaks of separately synthesized powders.

The average crystallite size, D_p, could be estimated from the Scherrer equation:

$$D_p = 0.9\lambda / (\beta \cos\theta) \quad (1)$$

where λ is the X-ray wavelength, β is the peak width at the half height after subtracting the instrumental line broadening, and θ is the Bragg angle of a diffraction peak. The most intense diffraction peak (112) was evaluated to compare the crystal sizes of all samples at <112> direction. Average sizes of 9.8 and 27.4 nm were obtained for the powders RT and HT, confirming the great effect of temperature on promoting crystal growth. However, the crystal sizes obviously decreased when the mineralization was carried out within kapok lumen: 5.0 and 11.8 nm for RT-24 and HT-24, respectively. This result may be due to the limited salts available inside the lumen or excessive nucleation sites on the inner wall, which suppressed the size of resultant crystals. The mineralization period over 6 hours did not obviously affect the crystal size at both room temperature and hydrothermal condition, as deduced from the equal β value between RT-6 and RT-24, HT-6 and HT-24.

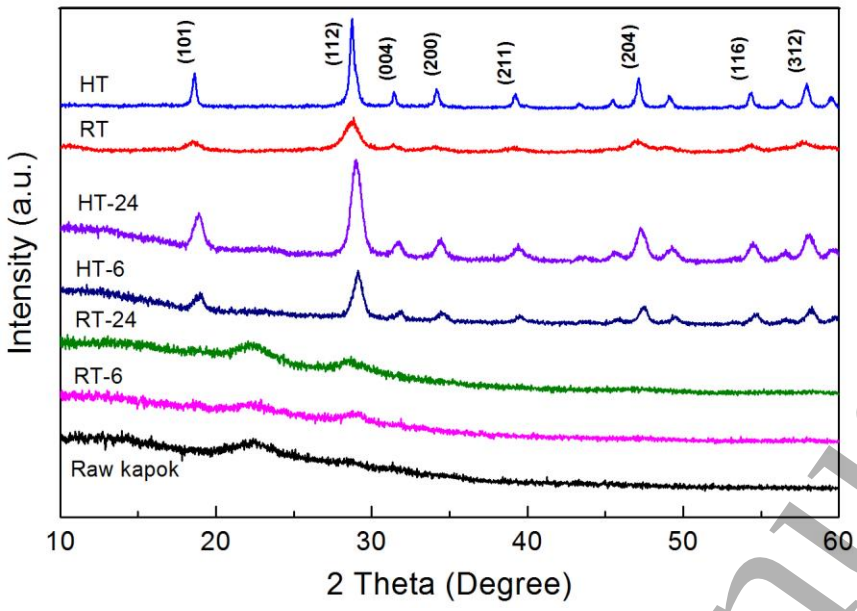

Figure 3. XRD patterns of tungstate powders and kapok fibers (raw and decorated).

In order to clarify the mineral content within kapok lumen, the raw and decorated fibers were analyzed by TGA (Figure 4). Two degradation steps were observed in all samples over the temperature range of 100 - 500 ^{o}C. As all the samples were completely dried before testing, no detectable weight loss was observed below 200 ^{o}C. The raw kapok fiber loses weight in such two stages: 200 - 300 ^{o}C and 300 - 400 ^{o}C. The 1st stage is associated with the thermal degradation of polysaccharides, i.e. cellulose and hemicelluloses.[36] A fast degradation of the cellulose and hemicellulose happened near 300 ^{o}C, which resulted in a large amount of gaseous products through the cleavage of glycosidic linkage, C-H, C-O, and C-C bonds, giving a weight loss close to 70 %. The second sharp weight loss occurred around 400 ^{o}C, which is most likely due to the pyrolysis of aromatic compounds including original lignin and unsaturated derivatives formed by the degradation at lower temperatures.[37] The weight loss around 30 % is consistent with the lignin content of over 20 % in kapok fiber.[30] In comparison, all the kapok fibers decorated

with tungstate crystals show obvious delay of the two degradation processes by 10 - 30 °C and evident increment in residue. From their residues at the final temperature of 500 °C, the mass ratio of tungstate / kapok is estimated as 15/85, 52/48, and 54/46 for RT-6, HT-6, and HT-24, respectively. These results are in accordance with the SEM and XRD results above: the hydrothermal treatment significantly increased the mineral amount, and the mineralization beyond 6 h contributed little to the crystal amount. The tungstate growth on kapok inner walls reached almost saturation within 6 h. This approach achieved a load of luminous particles over 100 wt%, being much higher than previously reported luminous composite fibers.[14-16]

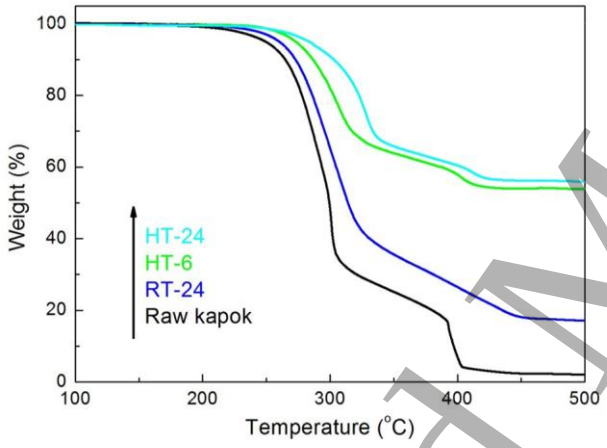

Figure 4. TGA curves of raw and decorated kapok fibers.

The luminescence spectra of samples prepared under room temperature and hydrothermal condition were presented in Figure 5. The excitation spectra of naked tungstate powders monitored at λ_{em} = 614 nm exhibit a broad band in the range of 230 – 310 nm. This broad excitation band with its peak around 274 nm mainly originates from the energy transitions from tungstate groups to Eu^{3+}, which has been approved by previous research.[28] Narrow peaks are observed beyond 300 nm (301, 319, 362, 382, 394, 416, 465 nm), ascribed to the electronic

excitation of Eu^{3+} 4f levels. The raw kapok fiber does not give any luminescence information. The decorated kapok fibers show a shift of the energy transition band from 274 to 261 nm, and present much weaker lines at 394 and 465 nm than the naked powders. This change cannot be attributed to the hindrance of kapok wall, since the kapok fiber has no any obvious absorbance peaks in these ranges (Figure S1). So far, the reason of the weakening narrow peaks has not been well explored yet.

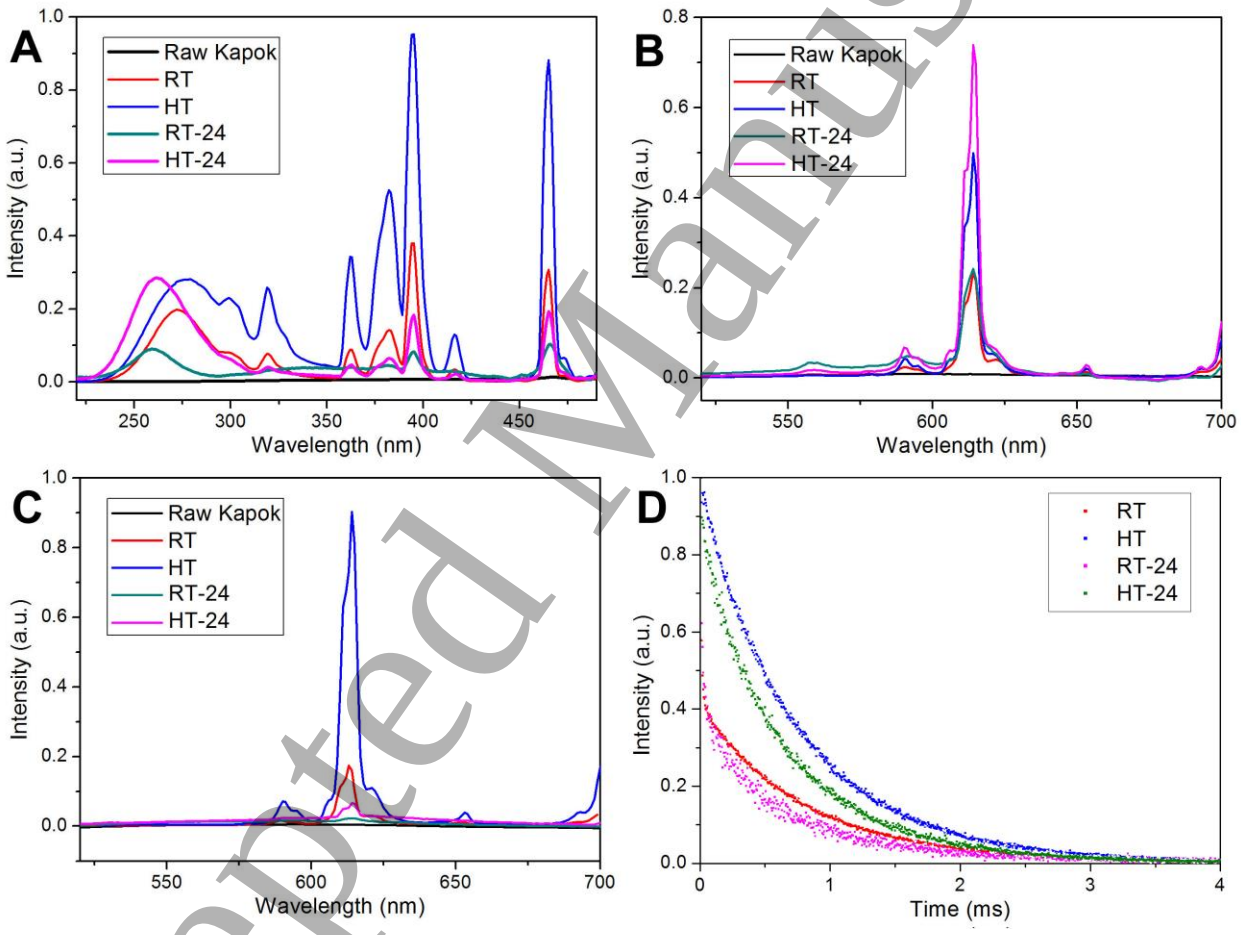

Figure 5. Phosphorescence properties of kapok fibers (raw and decorated RT-24, HT-24) and tungstate powders (RT, HT): (A) excitation spectra (λ_{em} = 614 nm), (B) emission spectra (λ_{ex} = 254 nm), (C) emission spectra (λ_{ex} = 365 nm), (D) luminescence decay curves.

Figure 5B and C demonstrated the emission characteristics of the as-prepared samples under the excitation of 254 and 365 nm, respectively. The emission spectra of naked powders exhibit three peaks centered at 591, 614 and 653 nm, approving the red luminescence under both excitation wavelengths. The electronic dipole transition of $^5D_0$ -- $^7F_2$ is characterized by a set of emissions at 606, 611, 614 and 622 nm that are not very narrow and overlap together. The $^5D_0$ -- $^7F_1$ line is observed at 591 nm, which originates from the parity-allowed magnetic dipole transition. The emission is dominated by the transition from $^5D_0$ to $^7F_2$ state with the most intensive peak at 614 nm in all samples excited with 254 nm UV, demonstrating the efficient energy transfer from WO_4^{2-} to Eu^{3+} in the crystals. The measured luminescence intensity is enhanced by hydrothermal process in both naked and capsulated particles, which is in a good agreement with the crystal size increment derived from XRD results. It should be noted that excitation at 254 nm induces comparable emissions from naked and capsulated crystals while excitation at 365 nm produces much weaker emission from the capsulated crystals. This result has been expected from their comparison in excitation spectra (Figure 5A).

The luminescence decay curves of the $^5D_0$ level in Figure 5D (under 254 nm excitation) exhibit multi-exponential feature that can be well reproduced with $R^2 > 0.99$ by a double-exponential function as $I = A_1exp(-t/\tau_1) + A_2exp(-t/\tau_2)$, where τ_1 and τ_2 are the fast and slow components of the luminescent lifetimes, and A_1 and A_2 are the fitting parameters, respectively. The double-exponential decay behavior of the activator is often observed when the excitation energy is transferred from the donor.[38] The average lifetimes of $^5D_0$ -- $^7F_2$ emission for Eu^{3+}, defined as $< \tau > = (A_{12}\tau_{12} + A_{22}\tau_{22})/(A_1\tau_1 + A_2\tau_2)$, were calculated to be 0.38, 0.63, 0.33 and 0.51 ms for samples RT, HT, RT-24 and HT-24, respectively. Hydrothermal process supports longer lifetimes, in agreement with their bigger crystal sizes calculated from XRD results. On the basis

of emission spectra and the lifetimes of $^5D_0$ emitting level, the luminescence quantum efficiency, η, for Eu^{3+} ions in $CaWO_4$ nanocrystals can be determined as 39%, 73%, 24% and 60% for samples RT, HT, RT-24 and HT-24. The crystals deposited within kapok fibers present a notable decrease in luminescence efficiency by about 13%.

Figure 6 illustrates the optical images of an as-prepared non-woven pattern of decorated kapok fiber HT-24 that was incorporated in a cotton textile substrate. Red luminescence is apparently observed in fibrous pattern as well as naked powders under UV stimulation of 254 nm. When the powders and HT-24 were both wetted by statically immersion in distilled water for 2 hours, the luminescence of naked powders became weaker while that of decorated kapok HT-24 did not change at all. The luminescent microtubes can retain their red phosphorescence very well in wet conditions, and may be easily incorporated into various textures of textiles, papers, and composites. They also support stability against rubbing since the phosphors are well capsulated inside lumens instead of being exposed on outer surfaces.

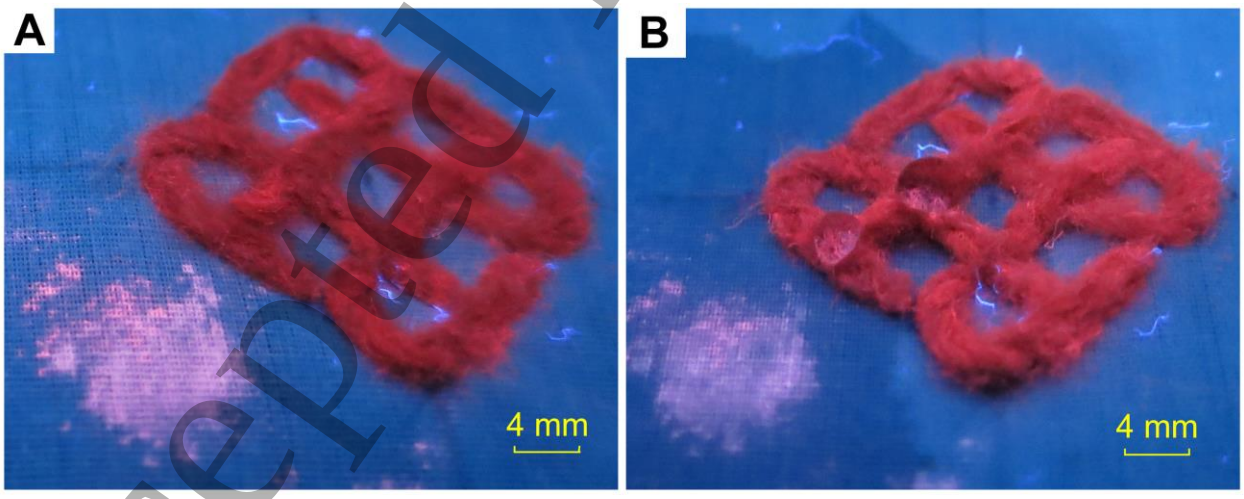

Figure 6. Photos of the HT powder (lower left corner) and nonwoven pattern composed of HT-24 fibers under 254 nm light: (A) dry state, (B) wet state.

4. CONCLUSION

A simple approach to fabricate luminous fibers was developed by growing the doped tungstate nanocrystals inside the kapok lumen. The fiber structures and luminescence properties were investigated, which indicated the enhancement of crystal growth and luminescence property by the hydrothermal condition. Though the introduction of kapok fiber showed no influence on tungstate crystal structure, it limited the excitation wavelength of tungstate crystals to only 254 nm instead of both 254 and 365 nm for naked crystals. These fibers were proved superior luminescence stability to naked powders in wet condition. This synthesis method provides an alternative and general way for preparing luminous fibers from natural materials. Such luminescent fibers with strong UV response have potential applications in the security marks of paper or textile products, and other flexible optical devices and sensors.

Supporting Information

The absorbance and reflectance spectra of pure kapok fibers are available in Figure S1.

ACKNOWLEDGEMENT

We sincerely acknowledge the supports from PolyU funds A-PL17, A-PM04, and 1-ZE27. We also thank Dr. Hongkai Wu's help with his reflection microscope.

REFERENCES

(1) Naddo, T.; Che, Y.; Zhang, W.; Balakrishnan, K. X. Y.; Yen, M.; Zhao, J.; Moore, J. S.; Zang, L. Detection of explosives with a fluorescent nanofibril film. *J. Am. Chem. Soc.* **2007**, 129, 6978−6979.

(2) Zang, L.; Che, Y.; Moore, J. S. One-dimensional self-assembly of planar π-conjugated molecules: adaptable building blocks for organic nanodevices. *Acc. Chem. Res.* **2008**, 41, 1596−1608.

(3) Strassert, C. A.; Chien, C. H.; Lopez, M. D. G.; Kourkoulos, D.; Hertel, D.; Meerholz, K.; De Cola, L. Switching on luminescence by the self-Assembly of a platinum (II) complex into gelating nanofibers and electroluminescent films. Angew. *Chem., Int. Ed.* **2011**, 50, 946−950.

(4) Yan, D.; Jones, W.; Fan, G.; Wei, M.; Evans, D. G. Organic microbelt array based on hydrogen-bond architecture showing polarized fluorescence and two-photon emission. *J. Mater. Chem. C.* **2013**, 1, 4138−4145.

(5) Magginia, L.; Bonifazi, D. Hierarchised luminescent organic architectures: design, synthesis, self-assembly, self-organisation and functions. *Chem. Soc. Rev.* **2012**, 41, 211−241.

(6) Holmes, J.D.; Johnston, K.P.; Doty, R.C.; Korgel, B.A. Control of thickness and orientation of solution-grown silicon nanowires. *Science.* **2000**, 287, 1471−1473.

(7) Liu, C.H.; Zapien, J.A.; Yao, Y.; Meng, X.M.; Lee, C.S.; Fan, S.S.; Lifshitz, Y.; Lee, S.T. High-density, ordered ultraviolet light-emitting ZnO nanowire arrays. *Adv. Mater.* **2003**, 15838−15841.

(8) 22Abid-Jarraya N, Turki-Guermazi H, Khemakhem K, Abid S, Saffon N, Fery-Forgues S. Investigations in the methoxy-iminocoumarin series: highly efficient photoluminescent dyes and easy preparation of green-emitting crystalline microfibers. Dyes and Pigments 2014; 101: 164-171.

(9) 22Gong P, Sun J, Xue P, Qian C, Zhang Z, Sun J, Lu R. Luminescent nanofibers fabricated from triphenylvinyl substituted carbazole derivatives via organogelation for sensing gaseous nitroaromatics. Dyes and Pigments 2015; 118: 27-36.

(10) O' Leary, L. E. R.; Fallas, J. A.; Bakota, E. L.; Kang, M. K.; Hartgerink, J. D. Multi-hierarchical self-assembly of a collagen mimetic peptide from triple helix to nanofibre and hydrogel. *Nat. Chem.* **2011**, 3, 821−828.

(11) Srinivasan, S.; Babu, P. A.; Mahesh, S.; Ajayaghosh, A. Reversible self-assembly of entrapped fluorescent gelators in polymerized styrene gel matrix: Erasable thermal imaging via recreation of supramolecular architectures. *J. Am. Chem. Soc.* **2009**, 131, 15122−15123.

(12) Yang, H.; Yi, T.; Zhou, Z.; Zhou, Y.; Wu, J.; Xu, M.; Li, F.; Huang, C. Switchable fluorescent organogels and mesomorphic superstructure based on naphthalene derivatives. *Langmuir* **2007**, 23, 8224-8230.

(13) Lv, N.; Dong, X.; Ma, Q. Parallel spinnerets electrospinning construct and properties of electrical-luminescent bifunctional bistrand-aligned nanobundles. *J. Mater. Sci.* **2014**, 49, 2171-2179.

(14) Yang, H.; Lightner, C.R.; Dong, L. Light-emitting coaxial nanofibers. *ACS Nano.* **2012**, 6622–6628.

(15) Guo, X.; Ge, M. The afterglow characteristics and trap level distribution of chromatic rare-earth luminous fiber. *Text. Res. J.* **2013**, 83, 1263-1272.

(16) Kulpinski, P.; Namyslak, M. Luminescent cellulose fibers activated by Eu^{3+}-doped nanoparticles. *Cellulose* **2012**, 19, 1271–1278.

(17) Mosinger, J.; Lang, K.; Plistil, L.; Jesenska, S.; Hostomsky, J.; Zelinger, Z.; Kubat, P. Fluorescent polyurethane nanofabrics: a source of singlet oxygen and oxygen sensing. *Langmuir* **2010**, 26, 10050–10056.

(18) Sommerdijk, N.A.J.M.; de With, G. Biomimetic CaCO3 mineralization using designer molecules and interfaces. *Chem. Rev.* **2008**, 108, 4499–4550.

(19) Gebauer, D.; Cölfen, H. Prenucleation clusters and non-classical nucleation. *Nano Today.* **2011**, 6, 6564–6584.

(20) Bleek, K.; Taubert, A. New developments in polymer-controlled, bioinspired calcium phosphate mineralization from aqueous solution. *Acta Biomater.* **2013**, 9, 6283–6321.

(21) Zhao, J.; Wei, Z.; Feng, X.; Miao, M.; Sun, L.; Cao, S.; Shi, L.; Fang, J. Luminescent and transparent nanopaper based on rare-earth up-converting nanoparticle grafted nanofibrillated cellulose derived from garlic skin. *ACS Appl. Mater. Interfaces.* **2014**, 6, 14945−14951.

(22) Tanaka, K.; Miyajima, T.; Shirai, N.; Zhang, Q.; Nakata, R. Laser photochemical ablation of $CdWO_4$ studied with the time-of-flight mass-spectrometric technique. *J. Appl. Phys.* **1995**, 77, 6581–6587.

(23) Mikhailik, V.B.; Kraus, H.; Wahl, D.; Itoh, M.; Koike, M.K.; Bailiff, I.K. One- and two-photon excited luminescence and band-gap assignment in $CaWO_4$. *Phys. Rev. B*. **2004**, 69, 205110.

(24) Mikhailik, V.B.; Bailiff, I.K.; Kraus, H.; Rodnyi, P.A.; Ninkovic, J. Two-photon excitation and luminescence of a $CaWO_4$ scintillator. *Radiat. Meas.* **2004**, 38, 585–588.

(25) Mikhailik, V. B.; Kraus, H.; Miller, G.; Mykhaylyk, M.S.; Wahl, D. Luminescence of $CaWO_4$, $CaMoO_4$, and $ZnWO_4$ scintillating crystals under different excitations. *J. Appl. Phys.* **2005**, 97, 83523.

(26) Min, K.W.; Mho, S.I.; Yeo, I.H. Electrochemical fabrication of luminescent $CaWO_4$ and $CaWO_4$: Pb films on W substrates with anodic potential pulses. *J. Electrochem. Soc.*, **1999**, 146, 3128–3133.

(27) Nazarov, M.V.; Tsukerblat, B.S.; Popovici, E.J.; Jeon, D.Y. Polarization selection rules for the allowed optical transitions in europium-terbium double activated calcium tungstate phosphor. *Solid State Commun.* **2005**, 133, 203–208.

(28) Su, Y.; Li, L.; Li, G. Synthesis and optimum luminescence of $CaWO_4$-based red phosphors with codoping of $Eu^{3+}$and Na^{+}. *Chem. Mater.* **2008**, 20, 6060–6067.

(29) Shi, M.; Xiao, H.; Yu, W. The fine structure of the kapok fiber. *Text. Res. J.* **2010**, 80, 159–165.

(30) Hori, K.; Flavier, M.E.; Kuga, S. Excellent oil absorbent kapok [Ceiba pentandra]L.) Gaertn.] fiber: fiber structure, chemical characteristics, and application. *J. Wood Sci.* **2000**, 46, 401–404.

(31) Zhang, X.; Fu, W.; Duan, C.; Xiao, H.; Shi, M.; Zhao, N.; Xu, J. Superhydrophobicity determines the buoyancy performance of kapok fiber aggregates. *Appl. Surf. Sci.* **2013**, 266, 225–229.

(32) Remgasamy, R.S.; Das, D.; Karan, C.P. Study of oil sorption behavior of filled and structured fiber assemblies made from polypropylene, kapok and milkweed fibers. *J. Hazard. Mater.* **2011**, 186, 526–532.

(33) Rahmah, A.R.; Abdullah, M.A. Evaluation of Malausian Ceiba pentandra (L.) Gaertn. for oily water filtration using factorial design. *Desalination* **2011**, 266, 51–55.

(34) Duan, C.; Zhao, N.; Yu, X. Chemically modified kapok fiber for fast adsorption of Pb^{2+}, Cd^{2+}, Cu^{2+} from aqueous solution. *Cellulose* **2013**, 20, 849–860.

(35) Yukawa, M.; Aoki, H.; Kuroda, A.; Maeda, S. Novel paper sheets containing kapok fibers. *NIP & Digital Fabrication Conference, 2013 International Conference on Digital Printing Technologies*. 257-260.

(36) Draman, S.F.S.; Daik, R.; Latif, F.A.; El-Sheikh, S.M. Characterization and thermal decomposition kinetics of kapok (Ceiba pentandra L.)-based cellulose. *Bioresource*s **2014**, 9, 8–23.

(37) Brebu, M.; Vasile, C. Thermal degradation of lignin – A review. *Cell. Chem. Technol.*, **2010**, 44, 353–363.

(38) Shen, W.Y.; Pang, M.L.; Lin, J.; Fang, J.Y. Host-sensitized luminescence of Dy^{3+} in nanocrystalline beta-Ga_2O_3 prepared by a Penchini-type sol-gel process. *J. Electrochem. Soc.* **2005**, 152, H25–H28.

TOC graphic